A Lateral Directional Flight Control System for the MOB Blended Wing Body Planform

Naveed U. Rahman* & James F. Whidborne*

* *Department of Aerospace Sciences, Cranfield University, Bedfordshire MK45 0AL, UK.*

Abstract: In this work, analysis and design of a lateral directional flight control system for a Blended Wing Body (BWB) aircraft is considered. The BWB configuration chosen for this purpose is the European MOB (Multidisciplinary Optimization Blended Wing Body) planform. The MOB configuration does not have vertical control surfaces for directional stability, instead small winglets with rudders are used. The lateral directional behavior of the baseline MOB configuration is analyzed and the inherent deficiencies both in terms of directional stability and control power are highlighted. A modification to this configuration is then proposed in which two vertical rudders are placed at the trailing edge of the center body. The improvement gained in the stability and directional stiffness is compared with the baseline configuration. The open loop analysis is followed by the design of a flight control system and verification of the results through non-linear simulations. It is concluded that the MOB configuration with winglet rudders does not have enough trim/control authority especially under asymmetric thrust conditions. Rudder control needs to be modified in order to make this a practical design.

Keywords: Stability Augmentation System, Blended Wing Body, Handling Qualities, Lateral Directional, Flight Control System.

NOMENCLATURE

S	Wing reference area, m^2
b	Wing span, m
c	Mean aerodynamic chord, m
m	Mass, kg
V_t	True airspeed, m/s
ρ	Air density, kg/m^3
M	Mach No
$\bar{q}$	Dynamic pressure, N/m^2
β	Angle of sideslip, rad
ϕ	Roll angle, rad
p	Roll rate , rad/s
r	Yaw rate, rad
ψ	Yaw angle, rad
u	Speed along X body axis, m/s
v	Speed along Y body axis, m/s
w	Speed along Z body axis, m/s
δa	Aileron deflection, rad
δe	Elevator deflection, rad
δr	Rudder deflection, rad
δt	Throttle

1. INTRODUCTION

In recent years the blended wing body configuration has been put forward by many researchers as the future environmental friendly aircraft. However this particular configuration poses many challenges to nearly all the disciplines in the aerospace industry, including structures, aerodynamics and flight controls. Very few tailless aircraft have been designed and flown successfully. This is especially true for the civil aerospace sector where the technical advantages associated with this design are easily outweighed by the requirements on safety and degradation in handling qualities. This degradation is the result of omission of a conventional horizontal and vertical stabilizer which reduces both directional and longitudinal static stability. In the military market however the tailless design has been more successful primarily due to its stealth characteristics and better payload carrying capability.

At Cranfield University the European MOB BWB planform was initially analyzed by Castro (2003) and later by Smith and Abbasi (2004). The present work will focus on the lateral directional axis to highlight its associated stability and control properties.

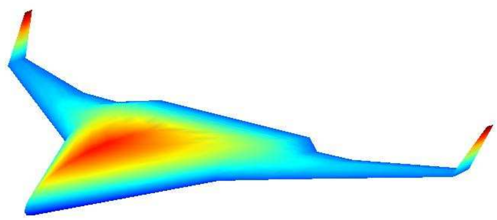

Fig. 1. MOB Configuration 1 - With winglet rudders

2. THE MOB BWB CONFIGURATION

The MOB BWB configuration is shown in Figure 1. The aircraft is tailless and the wing is blended smoothly into the fuselage. All the longitudinal and lateral controls are located on the trailing edge of the main lifting surface. Leibeck (2004) claims that such BWB configurations have a potential of superior aerodynamic performance especially under cruise conditions.

The control surface allocation is shown in Figure 2. A total of 13 flaps are located on the trailing edge and provide for both lateral and longitudinal control functions. With the exception of control surfaces 4/12, all the control surfaces on trailing edge are used as elevators. However, depending on the flight conditions the amount of roll control power or the number of control surfaces allocated for roll axis will vary. The rudder function is provided by flaps 1/15 and are located on the vertical fins at wing tips.

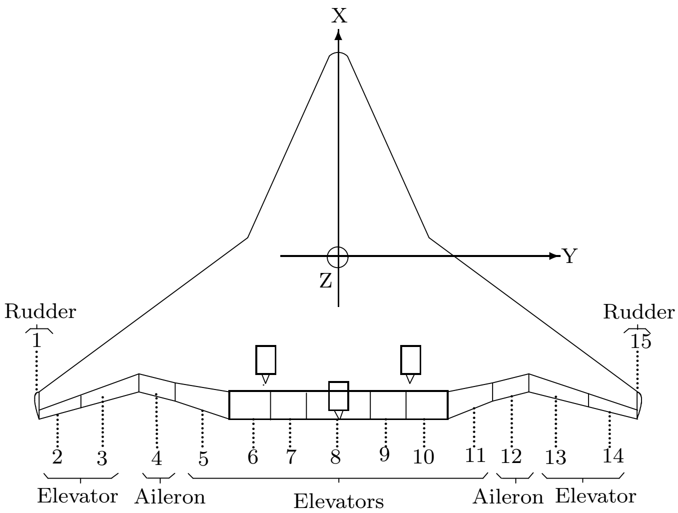

Fig. 2. Control Allocation on the BWB Tailless Aircraft

As a consequence of this configuration, the moment arm available for both longitudinal (pitch) and directional (yaw) control is much less than the conventional tailed aircraft. The obvious solution to this problem is to use a bigger control surface area to generate a larger control force. This can and has been done effectively for the elevators but not so conveniently for the rudders as there is simply not enough vertical surface area.

Parameter	Value	Units
Wing reference area, S	841.70	m^2
Wing span, b	80.00	m
Mean aerodynamic chord, c	12.31	m
Aircraft mass, m	371,280	kg
Inertia about X axis, I_{xx}	4.7032e07	kg-m^2
Inertia about Y axis, I_{yy}	2.5069e07	kg-m^2
Inertia about Z axis, I_{zz}	9.9734e07	kg-m^2

Table 1. BWB Aircraft Geometric and Mass properties

The geometric and mass specifications for the MOB BWB aircraft are presented in Table 1. It may be noted that these mass and inertias parameters are comparable to the Boeing 747 aircraft mass properties as stated in Hefley and Jewel (1982).

3. BWB - LATERAL DIRECTIONAL AERODYNAMICS

The BWB aerodynamic model used here is derived from the work done by Castro (2003). The non-dimensional aerodynamic coefficients are expressed in body axis and have been obtained through a combination of computational techniques and wind tunnel experiments. The lateral directional force and moment coefficients are outlined in (1) to (3).

$$C_y = C_{y_\beta}\beta + \frac{b}{V_t}\left(C_{y_r}r + C_{y_p}p\right) + C_{y_{\delta r}}\delta r \quad (1)$$

$$C_l = C_{l_\beta}\beta + \frac{b}{V_t}\left(C_{l_r}r + C_{l_p}p\right) + C_{l_{\delta r}}\delta r + C_{l_{\delta a}}\delta a \quad (2)$$

$$C_n = C_{n_\beta}\beta + \frac{b}{V_t}\left(C_{n_r}r + C_{n_p}p\right) + C_{n_{\delta r}}\delta r + C_{n_{\delta a}}\delta a \quad (3)$$

These non-dimensional aerodynamic coefficients are in general a function of angle of attack and center of gravity (CG) position. The values of these coefficients for a CG position of ($x_{cg} = 30.4\ m$) are given in Table 2.

Y Coefficients		L Coefficients		N Coefficients	
C_{y_β}	-0.2155	C_{l_β}	-0.1038	C_{n_β}	-0.0406
C_{y_r}	-0.1650	C_{l_r}	0.1366	C_{n_r}	-0.0178
C_{y_p}	-0.3122	C_{l_p}	-0.3420	C_{n_p}	-0.1490
$C_{y_{\delta r}}$	0.2335	$C_{l_{\delta r}}$	0.0780	$C_{n_{\delta r}}$	-0.0570
		$C_{l_{\delta a}}$	-0.0442	$C_{n_{\delta a}}$	0.0012

Table 2. Lateral Aero Coefficients, xcg = 30.4m

The side force along positive Y body axis and the roll/yaw moments about the X and Z axis respectively are given by (4) to (6).

$$Y = \bar{q}SC_y \quad (4)$$

$$L = \bar{q}SC_l b \quad (5)$$

$$N = \bar{q}SC_n b \quad (6)$$

4. BWB - TRIM ANALYSIS AND LINEAR MODEL

4.1 Trim Analysis

Trim analysis was performed by solving the equations of motion for a straight and level flight condition. The aircraft was trimmed by specifying a value of airspeed (V_t) and altitude (h) in the output vector. For a straight and level zero sideslip flight condition all the state derivatives are fixed at zero except the north position derivative ($\dot{p}_n$), which is allowed to vary. Although full six degree of freedom model with 12 state equations was used for the trim analysis, only the lateral directional axis will be considered. The lateral directional non-linear equations of motion which contribute to aircraft dynamics are

$$\begin{bmatrix} \dot{V} \\ \dot{p} \\ \dot{r} \\ \dot{\phi} \end{bmatrix} = \begin{bmatrix} Y/m + pW - rU - g\cos\theta\sin\phi \\ L/I_{xx} - qr(I_{zz} - I_{yy})/I_{xx} \\ (N + N_E)/I_{zz} - pq(I_{yy} - I_{xx})/I_{zz} \\ p + (q\sin\phi + r\cos\phi)\tan\theta \end{bmatrix}. \quad (7)$$

In the above, the term N_E, represents the yawing moment produced by the engine about the CG position. Nominally if all the three engines are operating at the same thrust level this yawing moment component should be zero. However, in an event of a starboard or port engine failure a significant yawing moment shall be produced which will have to be catered for by the rudder deflection.

To estimate the trim rudder requirements two trim cases were considered, (i) Engine Failure (asymmetric thrust) and (ii) Crosswinds. Trim requirements with an engine failure shall be considered here, however presence of cross-winds along with asymmetric thrust can further exacerbate the situation.

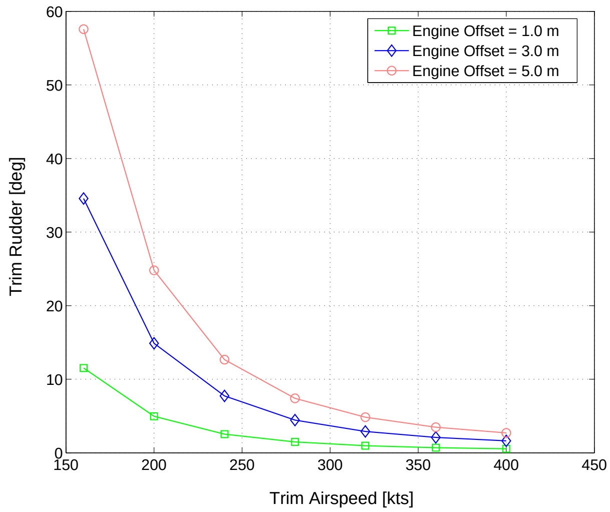

Fig. 3. MOB Config 1 - Trim Rudder - Asymmetric thrust

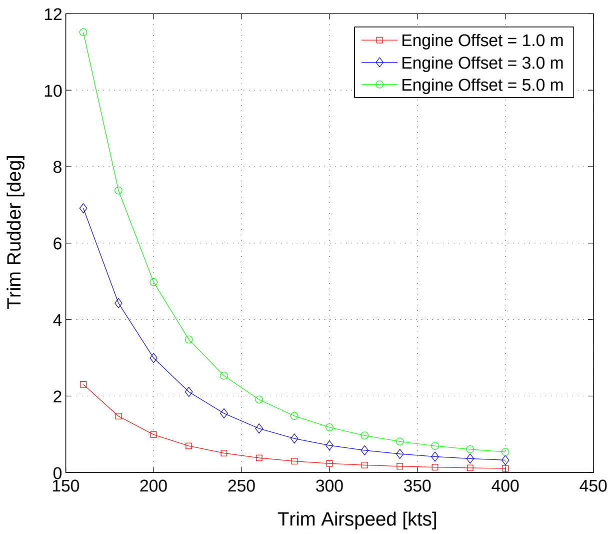

Fig. 4. MOB Config 2 - Trim Rudder - Asymmetric thrust

Figure 3 shows the rudder requirement for a starboard engine failure. At lower airspeeds and for a lateral engine offset of 5.0 m, the rudder deflection to achieve zero sideslip reaches very high values. Clearly the rudder control power is inadequate below 200 kts.

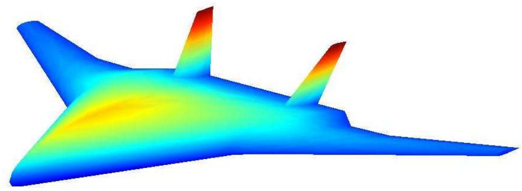

Fig. 5. MOB Configuration 2 - With increased Rudder power

In order to correct the weak rudder problem, Figure 5 shows a revised MOB configuration in which the rudder control power ($C_{n_\delta r}$) has been increased five times by utilization of twin vertical rudders. Trim results for this configuration are shown in Figure 4. The rudder deflections for the asymmetric thrust case are now within acceptable limits even at lower airspeeds. Such twin rudders on a BWB have the potential to provide an aerodynamic means of providing directional stability and control, however this comes at the cost of increased profile drag and weight due to the addition of the two vertical fins.

4.2 Linear Model and Open Loop Dynamics

For the linear analysis, the heading (ψ) and east position (p_E) states were omitted, while aileron (δa) and rudder (δr) controls were retained. From Cook (1997) the uncoupled lateral directional dynamics are

$$\begin{bmatrix} \dot{v} \\ \dot{p} \\ \dot{r} \\ \dot{\phi} \end{bmatrix} = \begin{bmatrix} Y_v & Y_p + W_1 & Y_r - U_1 & g\cos\theta_1 \\ L_v & L_p & L_r & 0 \\ N_v & N_p & N_r & 0 \\ 0 & 1 & \tan\theta_1 & 0 \end{bmatrix} + \begin{bmatrix} Y_{\delta a} & Y_{\delta r} \\ L_{\delta a} & L_{\delta r} \\ N_{\delta a} & N_{\delta r} \\ 0 & 0 \end{bmatrix} \begin{bmatrix} \delta a \\ \delta r \end{bmatrix} \quad (8)$$

The terms (U_1, W_1) are steady state X and Z axis body velocities, whereas (θ_1) is the trim pitch angle. Each element of the state and control matrix in (8) can be obtained by partial differentiation of the force and moment component in body axis w.r.t the appropriate state or control variable. The following expressions for the Y, L and N dimensional derivatives were used

$$\begin{bmatrix} Y_v \\ Y_p \\ Y_r \\ Y_{\delta a} \\ Y_{\delta r} \end{bmatrix} = \frac{\bar{q}S}{m} \begin{bmatrix} (1/V_t)C_{y_\beta} \\ (b/V_t)C_{y_p} \\ (b/V_t)C_{y_r} \\ C_{y_\delta a} \\ C_{y_\delta r} \end{bmatrix} \quad (9)$$

$$\begin{bmatrix} L_v \\ L_p \\ L_r \\ L_{\delta a} \\ L_{\delta r} \end{bmatrix} = \frac{\bar{q}Sb}{I_{xx}} \begin{bmatrix} (1/V_t)C_{l_\beta} \\ (b/V_t)C_{l_p} \\ (b/V_t)C_{l_r} \\ C_{l_\delta a} \\ C_{l_\delta r} \end{bmatrix} \quad (10)$$

$$\begin{bmatrix} N_v \\ N_p \\ N_r \\ N_{\delta a} \\ N_{\delta r} \end{bmatrix} = \frac{\bar{q}Sb}{I_{zz}} \begin{bmatrix} (1/V_t)C_{n_\beta} \\ (b/V_t)C_{n_p} \\ (b/V_t)C_{n_r} \\ C_{n_{\delta a}} \\ C_{n_{\delta r}} \end{bmatrix} \quad (11)$$

For a straight and level trim condition with an airspeed of ($V_t = 200\ kts$) and an altitude of ($h = 5,000\ ft$), the resulting state and controls matrix are

$$\begin{bmatrix} \dot{v} \\ \dot{p} \\ \dot{r} \\ \dot{\phi} \end{bmatrix} = \begin{bmatrix} -0.0247 & 22.392 & -102.66 & 9.624 \\ -0.0075 & -1.979 & 0.7907 & 0 \\ -0.0014 & -0.4071 & -0.0487 & 0 \\ 0 & 1.0000 & 0.1930 & 0 \end{bmatrix} \begin{bmatrix} v \\ p \\ r \\ \phi \end{bmatrix} +$$

$$\begin{bmatrix} -0.1038 & 0.5510 \\ -0.3293 & 0.1162 \\ 0.0043 & -0.0404 \\ 0 & 0 \end{bmatrix} \begin{bmatrix} \delta a \\ \delta r \end{bmatrix} \quad (12)$$

Using the above mathematical representation, linear models for the BWB aircraft were obtained for a range of CG positions and airspeeds.

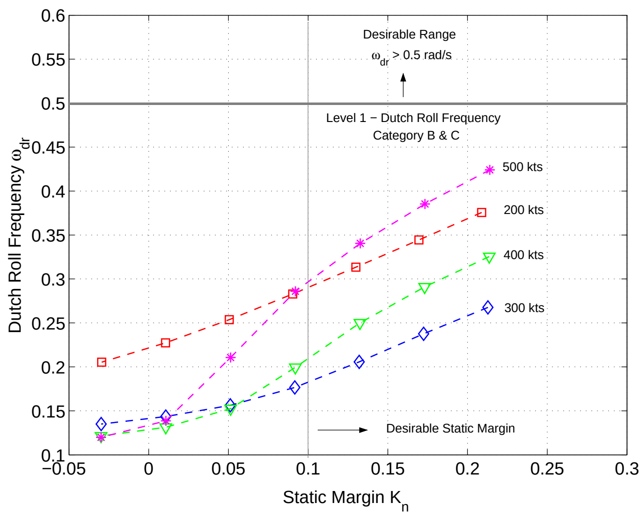

Fig. 6. Ducth Roll Damping (ω_{dr}) Vs. static margin

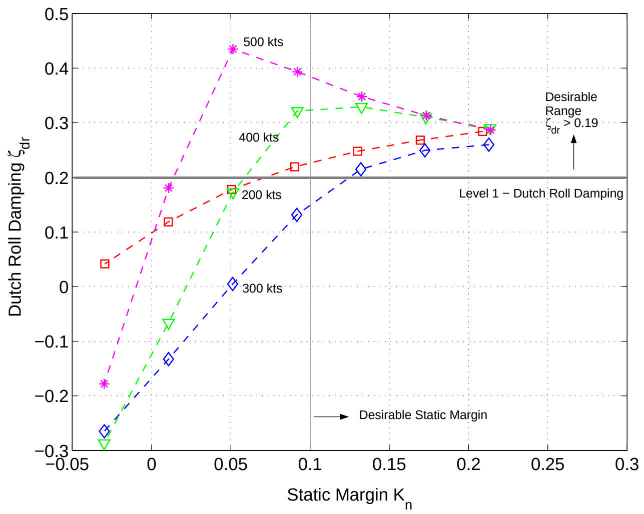

Fig. 7. Dutch Roll damping (ζ_{dr}) Vs. static margin

Figures 6 and 7 show the corresponding results for dutch roll natural frequency (ω_{dr}) and damping ratio (ζ_{dr}). Higher airspeeds and static margins tend to increase the dutch roll frequency but it still falls short of acceptable limits. For all combinations of speeds and CG positions the dutch roll mode is slower than the indicated MILSTD-8785C (1980) - Level I requirements. Figure 7 shows the corresponding dutch roll damping parameter . For static margins ($K_n > 0.1$), the dutch roll damping remains within acceptable Level I limits, however it deteriorates rapidly as the static margin is reduced further. A major contributor to this slow dutch roll mode is the weak yaw stiffness parameter (C_{n_β}). Thus absence of conventional rudders not only affects the yaw control authority but also the lateral-directional dynamics.

5. SIMULATION RESULTS

In the previous sections, trim analysis for lateral directional axis of the BWB aircraft was presented. It was argued that under cross winds or asymmetric thrust conditions the baseline MOB BWB configuration operating without the conventional rudders has inadequate rudder control power to trim the aircraft in the yaw axis. In this section this will be explored further by means of non-linear six degree of freedom aircraft flight simulations.

5.1 Lateral FCS Loop Structure

To run the non-linear simulation cases, a flight control system was designed for the baseline BWB configuration. Figure 8 shows the control system architecture. It comprises of two sections, (i) A lateral directional stability augmentation system and (ii) Offtrack and side-slip suppression system. The requirement was to maintain a specified ground track with zero sideslip, as required during take off or landing.

The stability augmentation system was designed so as to provide a consistent response to the pilot as the flight speed is varied. Due to poor directional stiffness there is a strong tendency of side slip generation and a roll/yaw cross coupling. In order to ensure turn coordination an aileron to rudder interconnect was used. Side slip feedback was necessary to speed up the very slow dutch roll mode. The washout time constant (τ_w) was chosen as 4.0 sec for damping the dutch roll mode. However even with this large value of washout time constant, the amount of dutch roll damping achieved was not greater than 0.5.

The side slip suppression loop was designed to ensure zero side slip under asymmetric thrust conditions, thus replacing the function of a pilot. An integral element was used in the forward path to ensure zero steady state slip. An offtrack control loop was designed to maintain a constant ground track. The offtrack loop is based on control of heading, which in turn demands a bank angle through gain K_ψ.

5.2 Gain Scheduling

Due to a large variation in dynamic pressure, the aerodynamic gains vary significantly. Hence it was necessary to schedule the gains of the flight control system. Table 3

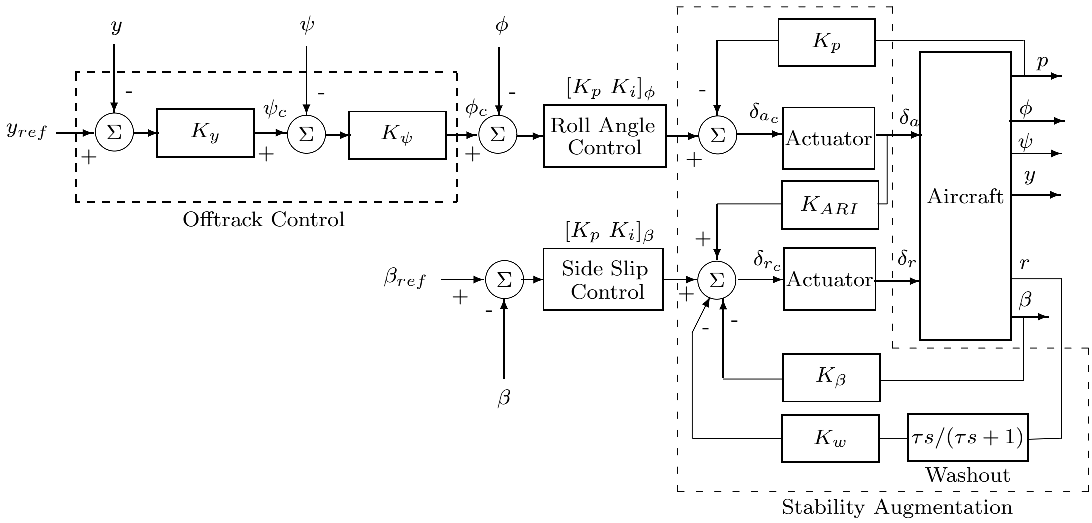

Fig. 8. Lateral FCS Loop Structure used for Non-linear simulation

shows a summary of lateral directional FCS gains as a function of dynamic pressure. Very high values of gains for aileron to rudder interconnect may be noted, with (K_{ARI}) exceeding 1.0 at low dynamic pressures. Thus, the baseline configuration requires almost requires the same amount of rudder as the amount of aileron to ensure a coordinated turn at low speeds. High values of yaw damping gains (K_w) are also noticeable. In addition a relatively large rudder saturation limit of ±37 deg was used.

$\bar{q}$	K_w	K_β	K_p	$[K_p]_\phi$	K_{ARI}
5000	-3.771	0.561	-1.512	-2.804	1.558
10000	-2.841	0.961	-0.680	-2.080	0.876
15000	-2.230	0.934	-0.224	-1.651	0.575
20000	-1.829	0.680	-0.039	-1.391	0.493
25000	-1.530	0.404	-0.022	-1.175	0.464

Table 3. Lateral FCS - Gain Schedule

5.3 Simulation Results with Engine Failure

The BWB aircraft was trimmed at a height of 10,000 ft and an airspeed of 200 kts. The initial off track distance (y) was set at -1000 m. Negative off track distance indicates that the aircraft is to left of the navigation track and vice versa. At 25 secs, the offtrack control system is activated, which causes the aircraft to bank to the right and brings the aircraft on zero offtrack within 100 secs. Figure 9 shows the time history.

With the side slip suppression system operative, the port engine failure was simulated at 100 sec. The asymmetric thrust generated by the starboard engine causes a negative yawing moment. The aircraft starts to generate a positive side slip. In order to suppress this side slip a negative rudder deflection is generated by the flight control system. On Figure 9 two time histories are plotted. The dashed line shows the aircraft response for the baseline configuration. The rudder quickly saturates at -37 deg, and the sideslip is not suppressed. The large of amount of sideslip generates a large roll moment causing ailerons to saturate as well. The aircraft thus diverges in both the roll and yaw axis. On the same figure results with five times the rudder power are also plotted. The aircraft now has enough rudder power to effectively maintain its flight path with zero side slip. Through out this analysis a lateral engine offset of 5.0 m was used along with thrust level of approx 430 KN.

5.4 Simulation Results with 30 knots Cross Wind

Figure 10 shows similar time histories for a 30 knots crosswind at 2000 ft and an approach airspeed of 165 knots. Although in this case the aircraft remains stable for both configurations the rudder is close to saturation for the baseline configuration.

6. CONCLUDING REMARKS

In this work, the lateral directional dynamics for the MOB Blended Wing body configuration were analyzed. Trimming analysis under asymmetric thrust conditions reveal that at low airspeeds consistent with that of takeoff and landing, the base line configuration with small winglet rudders does not have adequate control power to trim out the yawing moment generated by the engine. The rudder control power needs to be increased and a twin vertical rudder configuration is proposed. In the subsequent linear analysis and the design of the lateral directional flight control system it is also observed that the weak rudder is unable to effectively damp out the dutch roll mode. The gains required to achieve suitable yaw damping with the baseline configuration are unrealistic and would saturate the winglet rudders very quickly. Sideslip feedback was necessary to improve upon the directional stiffness and dutch roll frequency. The results were supported with non-linear simulations of asymmetric thrust and cross winds at approach airspeeds. For the twin rudder case the directional stiffness parameter ($C_{n\beta}$) was not modified, however this parameter is expected to increase with twin rudders thus ensuring a naturally higher directional stiffness. This

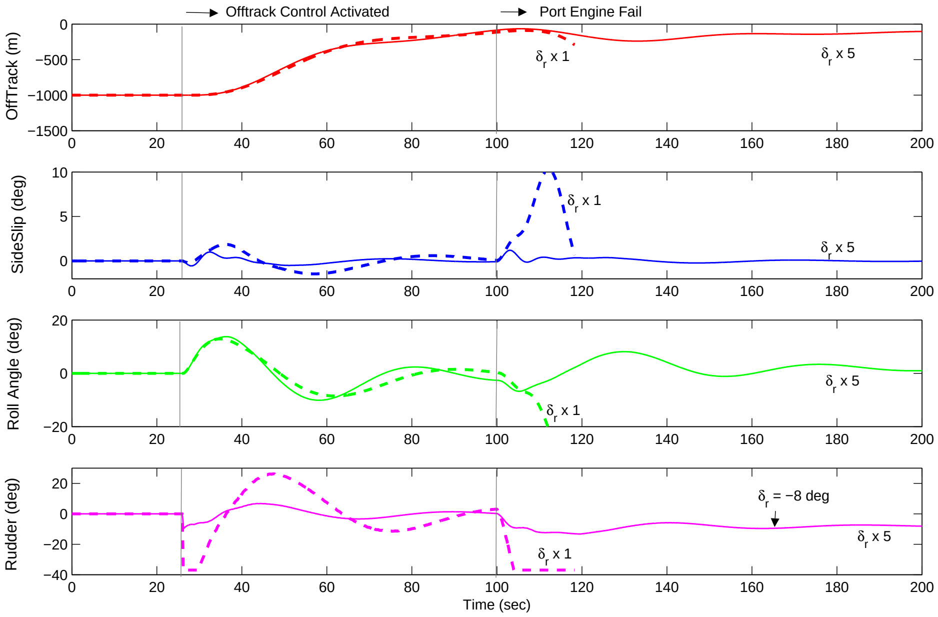

Fig. 9. Simulation Results - Port Engine Fail at 200 kts, 10000 ft

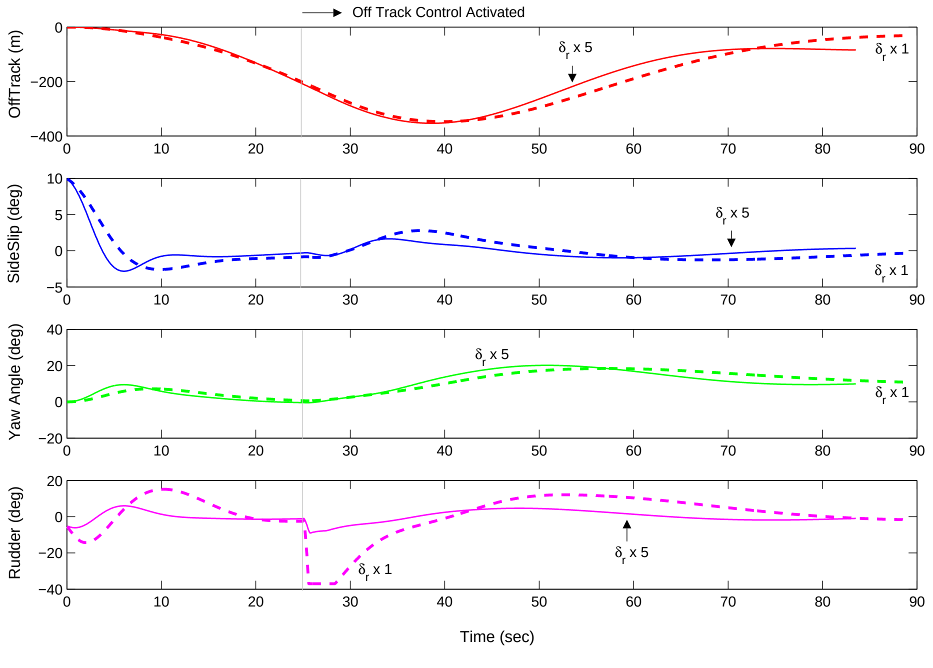

Fig. 10. Simulation Results - 30 Knots Cross Wind at 165 kts, 2000 ft

will have the beneficial effect of increased dutch roll frequency which in turn will allow a faster yaw rate washout network and smoother entry into turns.

REFERENCES

H. V. Castro. *Flying and Handling Qualities of a Fly by Wire Blended Wing Body Civil Transport Aircraft*. PhD thesis, Cranfield University, Cranfield UK, 2003.

M.V. Cook. *Flight dynamics principles*. Arnold publishers, 1997.

R.K. Hefley and W.F. Jewel. Aircraft handling qualities data nasa-cr-2144. Technical report, NASA, 1982.

R. Leibeck. Design of blended wing body subsonic transport. *Journal of Aircaft*, 41:10–25, 2004.

MILSTD-8785C. Military specification, flying qualities of piloted airplanes, MIL-F-8785C. Technical report, USAF, 1980.

H. Smith and Y. Abbasi. The MOB blended wing body reference aircraft, mob/4/cu/treport/004. Technical report, Cranfield University, UK, 2004.